

# Nonlinear screening and gas-liquid separation in suspensions of charged colloids

Bas Zoetekouw and René van Roij

*Institute for Theoretical Physics, Utrecht University, Leuvenlaan 4, 3584CE Utrecht, the Netherlands*

(Dated: September 9, 2018)

We calculate phase diagrams of charged colloidal spheres (valency  $Z$  and radius  $a$ ) in a 1:1 electrolyte from multi-centered nonlinear Poisson-Boltzmann theory. Our theory takes into account charge-renormalization of the colloidal interactions and volume terms due to many-body effects. For valencies as small as  $Z = 1$  and as large as  $10^4$  we find a gas-liquid spinodal instability in the colloid-salt phase diagram provided  $Z\lambda_B/a \gtrsim 24 \pm 1$ , where  $\lambda_B$  is the Bjerrum length.

Can like-charged colloids, dispersed in an aqueous solvent with monovalent cations and anions, spontaneously demix into a colloid-dilute “gas” phase and a colloid-dense “liquid” or “crystal” phase? For an index-matched solvent at room temperature, the answer to this question is *no* on the basis standard linear screening theory as formulated in the 1940s by Derjaguin, Landau, Verwey, and Overbeek (DLVO) [1, 2], but *yes* on the basis of some intriguing experimental observations in quasi-deionized suspensions of charged colloids [3–6].

The classic DLVO theory, which is a corner stone of colloid science, predicts that pairs of colloids of radius  $a$  and charge  $-Ze$  at separation  $r$  interact through a screened-Coulomb potential

$$v(r; Z, \kappa) = k_B T Z^2 \lambda_B \left( \frac{\exp[\kappa a]}{1 + \kappa a} \right)^2 \frac{\exp[-\kappa r]}{r}, \quad (1)$$

where the suspending medium is characterized by the temperature  $T$ , the Bjerrum length  $\lambda_B = e^2/(\epsilon k_B T)$  with the dielectric constant  $\epsilon$ , and the Debye screening length  $\kappa^{-1}$ . Here  $k_B$  is the Boltzmann constant and  $e$  the proton charge. The purely repulsive character of  $v(r)$  does not give rise to any cohesive energy to stabilize a dense liquid or crystal phase in coexistence with a much more dilute gas phase. Such cohesion effects, however, are observed in the experiments of Refs.[3–6]. They include, for instance, compressed crystal lattice spacings indicative of gas-crystal coexistence [3], gas-like voids in an otherwise homogeneous liquid-like suspension [4], long-lived metastable crystallites suggesting internal cohesion [5], and a (disputed) gas-liquid meniscus [6]. Explaining any of these phenomena requires cohesive energy, and the focus of much theoretical work has therefore been on extending DLVO theory to find “like-charge attraction”.

Important ingredients beyond DLVO theory are ion-ion correlations, nonlinear screening, and many-body effects. For (dilute) 1:1 electrolytes correlations are considered to be of only minor importance and will be ignored here, whereas the other two are important here. Nonlinear screening has been studied extensively in the context of (spherical) cell models, where the geometry allows for straightforward numerical solutions of the nonlinear Poisson-Boltzmann (PB) equation [7–10]. An important nonlinear effect is quasi-condensation of ions onto

a highly charged colloidal surface when  $Z\lambda_B/a \gtrsim 5 - 10$ . As a consequence, the colloidal charge that appears in the prefactor of Eq.(1) is renormalized from its bare value  $Z$  to a state point dependent  $Z^* < Z$ , i.e., the interactions are reduced but remain repulsive. Interestingly, free-energy calculations on the basis of the nonlinear cell model show *no* sign of a gas-liquid spinodal instability [9] either. On the basis of these results, together with, e.g., formal proofs [11] that nonlinear PB theory yields purely repulsive pair interactions, it is tempting to conclude that gas-liquid coexistence is impossible within (non)linear screening theory.

However, there are also studies that do show cohesion and gas-liquid spinodal instabilities. Examples include the early work by Langmuir [12], primitive model simulations of asymmetric electrolytes [13–15], PB calculations showing triplet attractions on top of pairwise repulsions [16] in agreement with experiments [17], and the extended Debye-Hückel theory and the boot-strap PB theory of Refs.[18, 19]. Interestingly, these systems have the explicit colloidal many-body character in common, as opposed to the cell geometry discussed above. Unfortunately, it is extremely time consuming and practically impossible to extend simulations such as those of Refs.[13–15] to realistic colloidal parameters (say,  $Z = 10^3 - 10^4$  with finite salt concentrations), or to calculate or measure effective  $n$ -body potentials with  $n \geq 4$ . Also attempts to study the full nonlinear many-body system, e.g., within the schemes as proposed in Refs.[20–22], turn out to be computationally difficult in the colloidal parameter regime. In fact, the colloidal parameter regime has so far mainly been studied as an explicit many-body system within *linear* screening theory, where the many-body character appears as a nontrivial density-dependence of pair interactions and as volume terms that can drive a gas-liquid transition [23–27], albeit mostly in regimes where charge renormalization should have been taken into account thereby stabilizing the suspension [25].

The key question addressed in this Letter is whether the intriguing and sometimes hotly-debated experiments like those of Refs.[3–6] can be explained by hard-core repulsions and Coulomb interactions only. This question is answered by calculating phase diagrams of the primitive model in the colloidal limit ( $Z \gg 1$  and point-

like cations and anions). We retain the best aspects of two well-established theories by combining the nonlinear screening effects of cell theory with the explicit many-body character of linear screening theory.

We consider  $N$  spherical colloids of hard-core radius  $a$  and fixed charge  $-Ze$  at positions  $\{\mathbf{R}_i\}$  in a solvent of dielectric constant  $\epsilon$  and volume  $V$  at temperature  $T$ . The system is in osmotic contact with a salt reservoir of monovalent point-like cations and anions at pair density  $2c_s$ , which gives rise to (yet unknown) ion concentrations  $c_{\pm}$  in the suspension. We only consider pairwise Coulomb and hard-core potentials between any pair of particles, such that contact distances are  $2a$ ,  $a$ , and  $0$  for a colloid–colloid, colloid–ion, and ion–ion pair, respectively. Thermodynamic properties and the phase diagram of this system can be determined once we explicitly know the semi-grand potential  $F(N, V, T, c_s)$ , which describes the colloids canonically and the ions grand-canonically, and which is defined by the partition function  $\exp[-\beta F] = (1/N!) \int_V d\mathbf{R}_1 \cdots d\mathbf{R}_N \exp[-\beta H\{\mathbf{R}\}]$ . Here  $\beta = 1/(k_B T)$  and  $H(\{\mathbf{R}\})$  is the effective colloid Hamiltonian. It was shown in Ref.[23] that  $H$  is the sum of the bare colloid–colloid interactions (hard-core and unscreened Coulomb) and the grand potential of the inhomogeneous fluid of cations and anions in the external field of the fixed colloidal charge distribution  $q(\mathbf{r}) = -Z \sum_{i=1}^N \delta(|\mathbf{r} - \mathbf{R}_i| - a)/4\pi a^2$ . Within mean-field theory, the effective Hamiltonian can be written as a sum of entropic and electrostatic-energy terms [23]

$$\beta H = \beta H_{\text{HS}} + \sum_{\alpha=\pm} \int d\mathbf{r} \rho_{\alpha}(\mathbf{r}) \left[ \ln \frac{\rho_{\alpha}(\mathbf{r})}{c_s} - 1 \right] + \frac{1}{2} \int d\mathbf{r} [\rho_+(\mathbf{r}) - \rho_-(\mathbf{r}) + q(\mathbf{r})] \phi(\mathbf{r}), \quad (2)$$

where  $H_{\text{HS}}$  denotes the hard-core interactions between the colloids, and where all  $\mathbf{r}$ -integrals are over the volume outside the colloidal cores:  $|\mathbf{r} - \mathbf{R}_i| \geq a$  for all  $i = 1, \dots, N$ . The yet unknown quantities are the equilibrium density profiles  $\rho_{\pm}(\mathbf{r}) = c_s \exp[\mp \phi(\mathbf{r})]$  of the cations and the anions, and the (dimensionless) electric potential  $\phi(\mathbf{r})$ . Note that  $\phi(\mathbf{r}) \equiv 0$  in the reservoir. These unknowns follow from Poisson's equation  $\nabla^2 \phi(\mathbf{r}) = -4\pi \lambda_B [\rho_+(\mathbf{r}) - \rho_-(\mathbf{r}) + q(\mathbf{r})]$ , which can be recast as the multi-centered non-linear PB equation

$$\nabla^2 \phi(\mathbf{r}) = \kappa^2 \sinh \phi(\mathbf{r}) \quad \mathbf{r} \text{ outside cores} \quad (3a)$$

$$\mathbf{n}_i \cdot \nabla \phi(\mathbf{r}) = Z \lambda_B / a^2 \quad \mathbf{r} = \mathbf{R}_i + a \mathbf{n}_i, \quad (3b)$$

where  $\kappa^{-1} = 1/\sqrt{8\pi \lambda_B c_s}$  is the reservoir's Debye screening length, and where  $\mathbf{n}_i$  is the unit surface normal of colloid  $i = 1, \dots, N$ .

In order to evaluate  $H$  of Eq.(2), we approximately solve Eqs.(3a)–(3b) as follows. We imagine each colloid  $i = 1, \dots, N$  in the center of a virtual cell of yet unknown radius  $b \geq a$ , and assume that the potential inside each

cell is spherically symmetric and given by  $\phi_c(|\mathbf{r} - \mathbf{R}_i|)$  for  $a < |\mathbf{r} - \mathbf{R}_i| < b$ . Denoting the net (yet-unknown) charge of the cell by  $Q$ , the cell-potential  $\phi_c(r)$  for  $a < r < b$  is the solution of the radially symmetric PB equation

$$\frac{1}{r^2} \frac{d}{dr} \left[ r^2 \frac{d}{dr} \phi_c(r) \right] = \kappa^2 \sinh \phi_c(r); \quad (4)$$

$$\phi'_c(a) = \frac{Z \lambda_B}{a^2}; \quad \phi'_c(b) = \frac{Q \lambda_B}{b^2}.$$

The boundary value problem (4) is easy to solve numerically on a radial grid for given  $\kappa$ ,  $b$ ,  $\lambda_B$ ,  $Z$  and  $Q$ . Outside the cells we retain the multi-centered character of  $\phi(\mathbf{r})$ , but we exploit that it varies only weakly from some spatial constant  $\bar{\phi}$  (provided  $b$  is large enough), such that  $\phi(\mathbf{r}) - \bar{\phi}$  is the small parameter in a linearized treatment of Eq.(3a). The linearized multi-centered PB equation can be solved analytically [23], and in terms of a (yet unknown) effective colloidal charge  $-Z^*e$  the resulting potential outside the cells is given by  $\phi(\mathbf{r}) = \bar{\phi} - \tanh \bar{\phi} + \sum_{i=1}^N \phi_1(|\mathbf{r} - \mathbf{R}_i|)$ , with the Yukawa “orbitals”

$$\phi_1(r) = -Z^* \lambda_B \frac{\exp(\bar{\kappa} a)}{1 + \bar{\kappa} a} \frac{\exp(-\bar{\kappa} r)}{r}. \quad (5)$$

Following Ref.[23], we identify  $\bar{\phi}$  with the Donnan potential of the renormalized system, such that  $\sinh \bar{\phi} = -Z^* n / (2c_s \exp[-\eta/(1-\eta)])$ , with  $n = N/V$  the colloid density and  $\eta = 4\pi a^3 n / 3$  the packing fraction. Hence also  $c_{\pm} = c_s \exp[\mp \bar{\phi}]$  and  $\bar{\kappa}^2 = 4\pi \lambda_B (c_+ + c_-)$  are known explicitly. Therefore,  $\phi(\mathbf{r})$  is completely determined inside and outside the cells once  $Q$ ,  $b$  and  $Z^*$  are specified.

How to determine these unknown quantities? In this Letter we calculate  $Q$  and  $Z^*$ , for a fixed  $b$  to be discussed below, by imposing continuity of the (average) potential and its gradient at the cell boundaries. Choosing the origin at  $\mathbf{R}_1$ , this implies that

$$\phi_c(b) = \bar{\phi} - \tanh \bar{\phi} + \phi_1(b) + \left\langle \sum_{i=2}^N \phi_1(|b \mathbf{n}_1 - \mathbf{R}_i|) \right\rangle; \quad (6a)$$

$$\phi'_c(b) = \phi'_1(b) + \left\langle \mathbf{n}_1 \cdot \nabla \sum_{i=2}^N \phi_1(|b \mathbf{n}_1 - \mathbf{R}_i|) \right\rangle. \quad (6b)$$

The angular brackets in the right hand side of Eq.(6a) indicate an average involving the colloid–colloid radial distribution function  $g(R)$ , and this term can be written as  $n \int d\mathbf{R} g(R) \phi_1(|b \hat{\mathbf{r}} - \mathbf{R}|)$ , and likewise for Eq.(6b). In principle one could think of setting up a scheme to calculate  $g(R)$  and the effective hamiltonian  $H(\{\mathbf{R}\})$  self-consistently, yet here we are satisfied with the crude approximation that  $g(R) = 0$  for  $R < 2b$  and  $1$  for  $R > 2b$ . This simplification allows for straightforward analytic expressions for the bracketed terms in Eqs.(6a) and (6b), which can then be easily solved numerically for the two unknowns  $Q$  and  $Z^*$  at fixed  $(Z, \lambda_B, a, b, \eta)$ .

The remaining problem is to choose the cell radius  $b$ . We checked that the largest physically reasonable choice,  $b = a\eta^{-1/3}$ , for which the cell has the volume of the Wigner-Seitz cell, yields essentially charge-neutral cells,  $Q/Z \ll 1$ , such that (i)  $Z^*$  is identical to Alexander's renormalized charge [7, 8], and (ii) *no* gas-liquid instability is expected [9]. One also easily checks that the smallest possible choice,  $b = a$ , ignores any nonlinearity and leads essentially to the volume-term theories of Refs.[23, 26, 27], which *do* predict gas-liquid spinodals. Our present choice for  $b$  is in between these two extremes, and is such that  $b$  is large enough for the region outside the cells to be properly described by linear screening, yet small enough to avoid significant overlaps of the cells. Moreover, since  $b$  is an unphysical parameter, the phase diagrams should not depend on  $b$ . All this is achieved, except perhaps in some extreme parameter regimes, by choosing  $b$  such that  $|\phi_c(b) - \bar{\phi}| = \delta$  (or  $b = a$  if  $Z\lambda_B/a$  is small enough), with fixed  $\delta \simeq 1$ . This criterion for  $b$  leads to values of  $b/a$  changing monotonically from  $b/a \rightarrow 1$  (linear screening) for high packing fractions ( $\eta > 0.5$ ) or high salt concentrations ( $\kappa a > 5$ ) to  $b/a > 10$  (nonlinear screening) for dilute systems ( $\eta \ll 10^{-3}$ ) at extremely low salt concentrations ( $\kappa a < 0.1$ ).

Our numerical results show that  $Z^*$  as defined by our procedure has all the characteristics of the renormalized charge as defined by Alexander[7], i.e.  $Z^* \simeq Z$  if  $Z\lambda_B/a \lesssim 5$ , if  $\kappa a$  is sufficiently large, or if  $\eta$  is high, and  $Z^* < Z$  otherwise. For instance, for  $Z = 1000$  and  $a = 100\lambda_B$  (which are of the order of the experiments of Refs.[31]), we find for  $\eta < 10^{-2}$  that  $Z^* \simeq 700, 900$  for  $\kappa a = 1, 5$ , respectively, and  $Z^*$  increases (in a non-monotonic fashion) to  $Z$  for increasing  $\eta$ . These effects, which are independent of  $\delta$  (and hence of  $b$ ) provided  $0.75 \leq \delta \leq 1.25$ , are also found in Alexander's traditional cell model [28] and in experiments [29].

With  $Q$  and  $Z^*$  determined from the continuity at the cell boundary (6a) and (6b), and  $b$  from the criterion as described above, the potential  $\phi(\mathbf{r})$ , and hence the ionic density profiles  $\rho_{\pm}(\mathbf{r})$ , are known explicitly, both inside and outside the cells. The Hamiltonian (2) can thus be evaluated explicitly. After tedious but straightforward calculation, in which the logarithmic terms are expanded to quadratic order outside the cells, one obtains

$$H(\{\mathbf{R}_i\}) = \Phi + \sum_{i < j}^N v(|\mathbf{R}_i - \mathbf{R}_j|; Z^* \sqrt{1 - \Upsilon(\bar{\kappa}a)}, \bar{\kappa}) \quad (7)$$

with a so-called volume term  $\Phi$  that does *not* depend on the coordinates of the colloids, and a sum of pairwise screened-Coulomb interactions (1) with an effective charge and an effective screening parameter. Here we introduced the function  $\Upsilon(x) = (1+x)(1-\exp[-2x])/2x$ , such that the factor  $\sqrt{1 - \Upsilon(\bar{\kappa}a)}$  in the effective charge is of order 1/2 in all but very extreme parameter regimes.

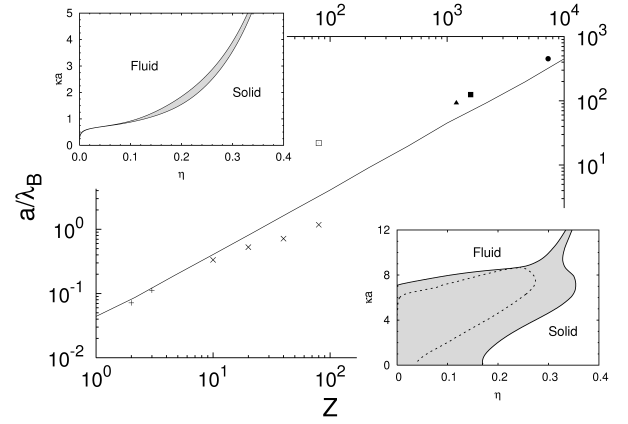


Figure 1: Typical  $\eta - \kappa a$  phase diagrams (insets) and critical line  $Z\lambda_B/a \sim 24 \pm 1$  (main figure), as determined over many decades of the parameters by the present theory, for suspensions of charged colloids (charge  $-Ze$ , radius  $a$ , packing fraction  $\eta$ ) in osmotic contact with a 1:1 electrolyte of reservoir screening constant  $\kappa$  and Bjerrum length  $\lambda_B$ . The critical line, which actually consists of three superimposed lines for  $\delta = 0.75, 1, 1.25$  (see text), separates the strong-coupling regime (lower right) *with* a spinodal gas-liquid instability (dashed line) and a large density gap (grey area) at fluid-solid coexistence for low  $\kappa a$  from the low-coupling regime (upper left part) *without* spinodal instability and with only a narrow density gap at fluid-solid coexistence. Criticality as found in the primitive model simulations of Refs.[13] and [14] are indicated by  $\times$  and  $+$ , respectively, the simulated state point of Ref.[32] without an instability is indicated by  $\square$ , and the experimental systems in which evidence for large density gaps at gas-liquid and gas-crystal coexistence was found are indicated by  $\blacktriangle$  [30],  $\blacksquare$  [31], and  $\bullet$  [5].

The volume term  $\Phi$  in Eq.(7) is given by

$$\begin{aligned} \frac{\beta\Phi}{V} = & 4\pi c_s n \int_a^b dr r^2 \{ \phi_c(r) \sinh \phi_c(r) - 2 \cosh \phi_c(r) \} \\ & - \frac{n}{2} Z \phi_c(a) + \frac{\eta}{1 - \eta} \frac{2c_+ c_-}{c_+ + c_-} \\ & + \left[ 1 - \eta \frac{b^3 - a^3}{a^3} \right] \left\{ \frac{n}{2} Z^* \bar{\phi} + \sum_{\alpha=\pm} c_\alpha \left[ \ln \frac{c_\alpha}{c_s} - 1 \right] \right\}. \end{aligned} \quad (8)$$

One easily checks that in the limit  $b \rightarrow a$ , for which  $Z^* \rightarrow Z$  and  $\phi_c(a) \rightarrow \bar{\phi} - \tanh \bar{\phi} + \phi_1(a) + \sum_{i=2}^N \phi_1(|a\mathbf{n}_i - \mathbf{R}_i|)$ , one recovers essentially the linear screening theory of Ref.[23], and that the first term of the second line of Eq.(8) contains the Debye-Hückel like  $-n^{3/2}$  cohesive energy (per unit volume) that drives the spinodal gas-liquid instability at low salinity [23, 26, 27].

With the Hamiltonian explicitly given by Eq.(7), we can calculate phase diagrams from  $F = \Phi + F_{\text{HSY}}$ , with  $F_{\text{HSY}}$  the free energy of a hard-sphere Yukawa fluid, which we calculate as in Ref.[23] by exploiting the Gibbs-Bogoliubov inequality. For fixed  $a/\lambda_B$  and  $Z$ , we calculate phase diagrams in the  $\eta - \kappa a$  representations by imposing equal osmotic pressure and chemical potential in

the coexisting phases. The insets of Fig.1 show two typical phase diagrams, calculated with  $\delta = 1$ , where the upper left corner ( $Z = 10$ ,  $a/\lambda_B = 100$ ) only shows crystallization with a narrow density gap, and the opposite corner ( $Z = 2000$ ,  $a/\lambda_B = 10$ ) exhibits a spinodal instability at low  $\kappa a$  and hence a large density gap between the coexisting phases. From many such phase diagrams we constructed a curve in the  $(Z, a/\lambda_B)$  plane of Fig.1, below which a spinodal instability is present in the  $\eta$ - $\kappa a$  plane. For  $\delta = 0.75, 1$ , and  $1.25$ , these curves superimpose on a single line that is well approximated by  $Z\lambda_B/a = 24 \pm 1$  over many decades of  $(Z, a/\lambda_B)$ . The independence of  $\delta$  confirms again that the phase diagrams are independent of the artificial cell radius  $b$  (provided  $b$  is chosen sensibly, i.e.  $\mathcal{O}(\delta) = 1$ ). The critical line from the linear screening theory,  $b = a$ , satisfies  $Z\lambda_B/a \simeq 6 - 7$  (not shown) for  $Z \geq 10$ , where the weaker critical coupling indicates that charge renormalization has a stabilizing effect on the suspension in agreement with Ref.[25].

Fig.1 also shows the parameters of three colloidal systems for which phase-instabilities have been observed experimentally (filled symbols in the figure); they are reasonably close to, yet systematically above, our predicted critical line, by a factor of 1.5-2. Our critical line also shows good agreement with (estimates of) critical points in the salt-free primitive model simulations of Refs. [13, 14] for  $10 \leq Z \leq 80$  ( $\times$ ) and  $Z = 2, 3$  ( $+$ ), respectively, although a systematically increasing deviation up to a factor  $\sim 3$  (for  $Z = 80$ ) is obscured by the double logarithmic scale of Fig.1. This deviation could perhaps be explained by the fact that for close-to-critical values of  $Z\lambda_B/a$ , instabilities (detached from the freezing line) first appear at  $\kappa a = 0$  but only for extremely dilute systems ( $\eta \ll 10^{-3}$ , decreasing with increasing  $Z$ ), while the lowest density considered in Ref.[13] is as "high" as  $\eta = 0.00125$ ; the instability reaches this state point at a coupling that increases with  $Z$  [33]. Note also that for  $Z = 1$ , our theory predicts the critical point at  $a/\lambda_B \approx 0.048$ , which is close to the well-known critical point of the symmetric 1:1 electrolyte at  $a/\lambda_B = 0.057$  [34]. It is perhaps surprising, yet comforting, that the critical point as predicted by the present theory, which is "designed" to deal with  $Z \gg 1$ , agrees quantitatively with the primitive model simulations of in the low-valency regime  $Z \leq 10$ .

To conclude, we have constructed a theory for colloidal suspensions that interpolates between the well known limits of linear DLVO-type and non-linear cell-type PB theories, thereby combining the multi-centered character and the volume terms of the former with the charge renormalization of the latter. For high enough charges and small enough radii ( $Z\lambda_B/a \gtrsim 24 \pm 1$ , i.e. well into the charge renormalization regime), we find spinodal instabilities at low ionic strengths. The theory directly extends the undisputed gas-liquid instability for asymmetric low-valency electrolytes ( $Z \leq 10$ ) to the colloidal regime

( $Z \gtrsim 1000$ ), although the existing experimental evidence in the colloidal regime is at somewhat weaker couplings than required according to our predictions here. We are currently extending the present theory to take charge regulation into account, in order to investigate whether the required coupling can be shifted towards experimentally realized systems. Alternatively it is interesting to consider the possibility that the experimentally determined "effective" colloid charge should not be identified with  $Z$  (as we did here) but with a renormalized charge [35], as this would shift the experimental points of Fig.1 closer to or beyond the critical line predicted here.

We thank Marjolein Dijkstra for useful discussions. This work is part of the research programme of the "Stichting voor Fundamenteel Onderzoek der Materie (FOM)", which is financially supported by the "Nederlandse Organisatie voor Wetenschappelijk Onderzoek (NWO)".

- 
- [1] B. Derjaguin and L. Landau, *Acta Physicochim.*, URSS **14**, 633 (1941).
  - [2] J. W. Verwey and J. T. G. Overbeek, *Theory of the stability of lyotropic colloids* (Elsevier, Amsterdam, 1948).
  - [3] N. Ise, T. Okubo, M. Sugimura, K. Ito, and H. Nolte, *J. Chem. Phys.* **78**, 536 (1983).
  - [4] K. Ito, H. Yoshida, and N. Ise, *Science* **263**, 66 (1994); but see L. Belloni, *J. Phys. Condens. Matter* **12**, R549 (2000).
  - [5] A. E. Larsen and D. G. Grier, *Nature* **385**, 230 (1997).
  - [6] B. V. R. Tata *et al*, *Phys. Rev. Lett.* **69**, 3778 (1992); T. Palberg and M. Würth, *Phys. Rev. Lett.* **72**, 786 (1994).
  - [7] S. Alexander *et al*, *J. Chem. Phys.* **80**, 5776 (1984).
  - [8] E. Trizac *et al*, *Langmuir* **19**, 4027 (2003).
  - [9] H. H. von Grünberg *et al*, *Europhys. Lett.* **55**, 580 (2001).
  - [10] Y. Levin *et al*, *J. Phys.: Condens. Matter* **15**, S3523 (2003).
  - [11] J. C. Neu, *Phys. Rev. Lett.* **82**, 1072 (1999); E. Trizac and J.-L. Raimbault, *Phys. Rev. E* **60**, 6530 (1999).
  - [12] I. Langmuir *J. Chem. Phys.* **6**, 873 (1938).
  - [13] P. Linse, *J. Chem. Phys.* **113**, 4359 (2000).
  - [14] A. Z. Panagiotopoulos and M. E. Fisher, *Phys. Rev. Lett.* **88**, 045701 (2002).
  - [15] A.-P. Hynninen *et al*, *J. Chem. Phys.* **123**, 084903 (2005).
  - [16] C. Russ *et al*, *Phys. Rev. E* **66**, 011402 (2002).
  - [17] C. Russ *et al*, *Europhys. Lett.* **69**, 468 (2005); *J. Phys.: Condens. Matter* **15**, S3509 (2003).
  - [18] D.Y.C. Chan *et al*, *Langmuir* **17**, 4202 (2001).
  - [19] S.N. Petris *et al*, *J. Chem. Phys.* **118**, 5248 (2003).
  - [20] M. Fushiki, *J. Chem. Phys.* **97**, 6700 (1992).
  - [21] J. Dobnikar *et al*, *J. Chem. Phys.* **119**, 4971 (2003).
  - [22] H. Löwen *et al*, *Phys. Rev. Lett.* **68**, 1081 (1992).
  - [23] B. Zoetelouw and R. van Roij, *Phys. Rev. E* **73**, 021403 (2006); R. van Roij *et al*, *Phys. Rev. E* **59**, 2010 (1999). R. van Roij and J.-P. Hansen, *Phys. Rev. Lett.* **79**, 3082 (1997).
  - [24] B. Beresford-Smith *et al.*, *J. Colloid Interface Sci.* **105**, 216 (1985).
  - [25] A. Diehl *et al.*, *Europhys. Lett.* **53**, 86 (2001).

- [26] P. B. Warren, J. Chem. Phys. **112**, 4683 (2000); Phys. Rev. E **73**, 011411 (2006).
- [27] A. R. Denton, Phys. Rev. E **62**, 3855 (2000); Phys. Rev. E **70**, 031404 (2004); Phys. Rev. E **73**, 041407 (2006).
- [28] L. Belloni, Coll. Surf. A **140**, 227 (1997).
- [29] L. Shapran *et al*, Coll. Surf. A **270**, 220 (2005).
- [30] Y. Monovoukas and A. P. Gast, J. Colloid Interface Sci. **128**, 533 (1989).
- [31] B. V. R. Tata *et al*, Phys. Rev. Lett. **78**, 2660 (1997); H. Yoshida *et al*, Langmuir **15**, 2684 (1999).
- [32] A.-P. Hynninen, and M. Dijkstra, J. Chem. Phys. **123**, 244902 (2005).
- [33] B. Zoetekouw, and R. van Roij, *in preparation*.
- [34] V. McGahay, and M. Tomozawa, J. Chem. Phys. **97**, 2609 (1992); M. E. Fisher, and Y. Levin, Phys. Rev. Lett. **71**, 3826 (1993).
- [35] P. Wette *et al*, J. Chem. Phys. **116**, 10981 (2002).